This is an *Accepted Manuscript*, which has been through the Royal Society of Chemistry peer review process and has been accepted for publication.

Accepted Manuscripts are published online shortly after acceptance, before technical editing, formatting and proof reading. Using this free service, authors can make their results available to the community, in citable form, before we publish the edited article. We will replace this *Accepted Manuscript* with the edited and formatted *Advance Article* as soon as it is available.

You can find more information about *Accepted Manuscripts* in the **Information for Authors**.

Journal Name

ARTICLE TYPE

An exceptionally stable functionalized metal-organic framework for lithium storage

Yichao Lin, Qiuju Zhang, Chongchong Zhao, Huailong Li, Chunlong Kong,* Cai Shen* and Liang Chen*

We present a designed synthesis of functionalized metal-organic framework with hydrophobic and polar functionalities, which exhibits remarkable thermal and chemical stability. The functionality and porosity make it a promising candidate in the application of Li-ion battery electrode.

Metal-organic frameworks (MOFs) are a class of porous materials that have received tremendous attentions due to their remarkable properties, structural and chemical versatility and tailorability.[1] The rational design of their structures may enable promising applications in gas storage,[2] Li storage,[3] and catalysis.[4] However, the thermal and chemical stability, which is highly demanded in practical applications, is usually the major drawback of many MOFs.[5] In particular, many types of MOFs are unstable in moisture, which can attack the metal connectors within MOFs, resulting in the phase transformation and decomposition of the frameworks.[6] In the complex working conditions, for example, in the electrochemical environment of Li-ion battery electrodes, the stability of MOFs is even worse.[3b,c,d] Fortunately, one of the most attractive traits of MOFs is their structural tunability, therefore, affording an opportunity to rationally select appropriate framework components to enhance the stability and performance.[7]

Recently, several studies have demonstrated that it is possible to build stable MOFs by post-synthetic modification of their frameworks with hydrophobic functionalities.[8] On the other hand, the inner pores can be functionalized by chemical grafting of the polar functionalities that can interact strongly with guest atoms or molecules.[9] Inspired by these studies, we propose to construct bifunctionalized MOFs (BMOF) with both hydrophobic and polar functionalities, which is expected to exhibit high stability as well as other desired properties. Herein we report the designed synthesis of a new BMOF with the phenyl and amine functionalities. The as-synthesized microporous BMOF shows exceptional chemical and thermal stability, and posesses reversible Li ion charge/discharge capacity.

Imidazole (IM) is an ideal building unit owing to the strong coordination between the N atoms and metal nodes (e.g., Zn).[10] Phenyl is a hydrophobic and rigid group so that it may impart excellent thermal and chemical stability to the resulting frameworks. Based on the density functional theory (DFT) calculations, we found that the amine groups can also serve as the binding sites to store Li atoms (Fig. S1). In addtion, the N atoms in IM can interact strongly with Li atoms. Therefore, we chose 2-aminobenzimidazole (abIM) as the organic linker because of the combination of phenyl, amine and imidazolate groups. However, we found that abIM and zinc nitrate hexahydrate failed to form any MOF products. Instead, we introduced the mixture of IM and abIM in order to induce the formation of frameworks. In the course of the systematic investigation of the formation of this new BMOF, high-throughput experiments were performed with various chemical and process parameters.[11] We systematically studied the influences of the molar ratios of starting compounds, the reaction temperatures, and reaction time on the product formation. A well-crystallized BMOF crystal with hybrid linkers was obtained by the reaction of IM and abIM (3:1), and zinc nitrate hexahydrate in N, N-dimethylformamide (DMF) solution at 130 °C for 72 h under autogenous pressure.
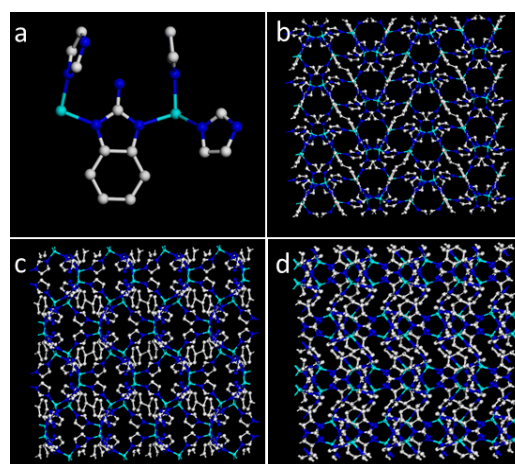

Fig. 1 The structure of BMOF: (a) the coordination environment of the Zn^{2+} ion and ligands. (b-d) the structure of BMOF viewed along *a* axis (b), *b* axis (c) and *c* axis (d). Color scheme: Zn-light blue; N-blue; C- white.

The as-synthesized BMOF crystal was structurally characterized and formulated by single-crystal X-ray diffraction (XRD) studies as $Zn(IM)_{1.5}(abIM)_{0.5}$. The compound crystallizes in the trigonal space group *Pbca* with

two zinc ions, one abIM and three IM ligands included in an asymmetric unit to form an infinite three-dimensional (3-D) framework (Fig. 1). Each Zn ion is coordinated in tetrahedral geometry with four N atoms from three different IM ligands and one abIM ligand. Each IM ligand bridges between two Zn nodes and thus constructs square channels along the *b* axis. These layered structures further align parallelly with each other through abIM ligands, forming 3-D frameworks. The amine and phenyl groups are located around the cavities, which polarize and functionalize the inner pores.
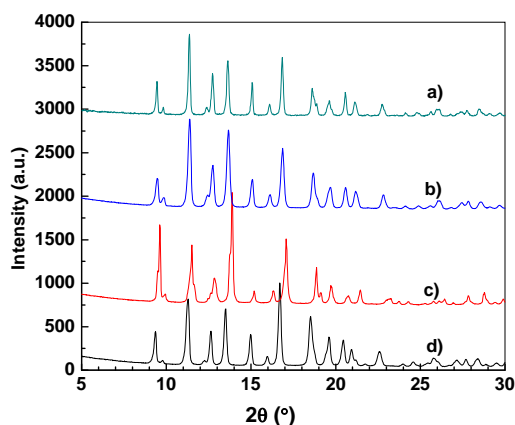

Fig. 2 Powder XRD patterns of the as-synthesized BMOF (a) and it immersed in water (b), acetone (c) and ethanol (d) at 333 K for 15 days, respectively.

Transmission electron microscopy (TEM) clearly indicates that a well-crystallized BMOF crystal was successfully synthesized (Fig. S2). Furthermore, X-ray photoelectron spectroscopy (XPS) and powder XRD patterns show a pure phase of the bulky sample (Fig. S3). Infrared spectra (IR) analysis distinctly shows the double peaks at 3490 cm^{-1} and 3380 cm^{-1}, which are ascribed to the asymmetrical and symmetrical stretching vibration of the amine groups (Fig. S4).[12] The sample was analyzed by ^{13}C solid-state nuclear magnetic resonance (NMR) (Fig. S5), which clearly shows the signals of IM and abIM. To further determine the pore structure and surface area of as-synthesized BMOF, N$_2$ adsorption-desorption isotherms were measured at 77.3 K (Fig. S6). The adsorption isotherm shows a very sharp uptake at P/P$_0$ from 10^{-5} to 10^{-1}, which is a signature feature of microporous materials.[13] The corresponding Brunauer-Emmett-Teller (BET) and Langmuir surface areas were calculated to be 821 and 1134 m$^2 \cdot$g^{-1}, respectively.

To evaluate the stability of as-synthesized BMOF, thermogravimetric (TG) analysis measurements were performed and shown in Fig. S7. Results indicate a loss of water and DMF up to 200 °C. It is noteworthy that the thermal stability of as-synthesized BMOF is remarkable with a decomposition temperature above 550 °C in both nitrogen and air. The decomposition temperature is much higher than that of most MOFs (particularly the amine-functionalized MOFs), which are commonly lower than 400 °C.[2d,14] However, we are aware that the TG analysis cannot fully reflect the thermal stability in practical applications due to the short testing duration. Therefore, we further evaluated the thermal stability

by heating the BMOF samples at 200 ^{o}C in air. We found that the structure of BMOF was well retained even after three days (Fig. S8). Along with the remarkable thermal stability, the BMOF displays exceptional chemical stability in water and organic solvents at 60 °C for 15 days. As shown in Fig. 2, the powder XRD patterns recorded for BMOF after such extensive treatment are unchanged. This is particuraly advangetous since many developed MOFs are extremely water-sensitive, resulting in the decomposition of the frameworks.[6]
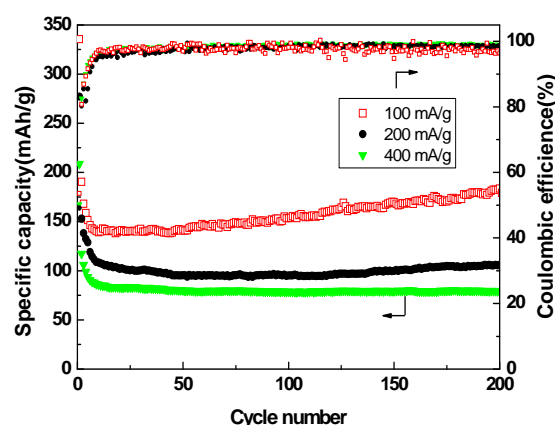

Fig. 3 Cycling performance and coulombic efficiency of the electrodes made with BMOF. The discharge process was carried out at various current densities of 100 mA/g, 200 mA/g and 400 mA/g.

Based on the DFT calculations, we expect that the BMOF may have an excellent reversible Li charge/discharge capacity. There are four potential sites in abIM for Li storage, including IM ring, beneze ring and IM ring in abIM, and amine group (Fig. S1). Fig. 3 displays the cycling performance and coulombic efficiency of the anodes made with the BMOF discharged at varying current densities of 100 mA/g, 200 mA/g, and 400 mA/g. Under all conditions, the specific capacity of BMOF stabilized after the 10th cycles, and no capacity loss was observed thereafter (200 cycles). For BMOF discharged at current density of 100 mA/g, at 200 cycles, the capacity even increased back to ~190 mAh/g, equal to the capacity of the second cycle. The columbic efficiencies (defined as the ratio of charge capacity to discharge capacity) all approach ~97% after the 10th cycles. It is noted that the higher columbic efficiency can be obtained at higher current density. A columbic efficiency of almost 100% was obtained for the sample discharged at a current density of 400 mA/g after 200 cycles. These results demonstrated the rapid kinetics during the cycling. Fig. S9 displays the discharge/charge profiles of the electrodes made with BMOF. There is a large irreversible capacity in the initial cycle, which can be ascribed to the solid electrolyte interface (SEI) formation. The formation of SEI limits further electrolyte decomposition to improve the cycle life performance of the cell.

To further prove the excellent performance of this new BMOF electrode, rate cycling performance was tested. As shown in Fig. 4, a highly symmetric pattern was obtained for the BMOF electrode discharged at various current densities (except for the first cycle due to the irreversible capacity loss).

Such highly symmetric pattern demonstrates the facile ion diffusion in the inter-connected 3D channels as well as the robustness of the MOF structure even under high-rate cycling. Indeed, the XRD of BMOF after 200 charge/discharge cycles

5 was identical to that of original BMOF, indicating the excellent stability of BMOF in the electrochemical conditions (Fig. S10). MOFs have been investigated for Li storage, some of which[3c,d] even exhibited high reversible capacities up to 560 mAh/g at 60 mA/g. However, after the discharge/charge

10 process, these MOF structures were decomposed or collapsed.[3b,c,d] Hence, it is the resulting solids (possibly metal oxides or carbon) that are responsible for the Li storage instead of the MOF. To date, only the mixed-valence Fe-MIL-53 was reported to be stable under the electrochemical

15 condition of Li-ion battery with a reversible capacity of 75 mAh/g at ~3mA/g. The Fe(III)/Fe(II) transformation during the discharge/charge process was proposed as the working mechanism for Li storage. In contrast to these reported MOFs, BMOF shows a reversible Li storage capacity (190 mAh/g) at

20 100 mA/g with a different working mechanism. Based on the DFT calculations (Fig. S1) and XRD (Fig. S10), we propose that Li is indeed stored within the BMOF pores as the frameworks remained intact during the discharge and charge process. The host-guest interactions between Li and amine

25 groups/N atoms in IM plays an important role in the storage capacity. Indeed, for IM and abIM precursors without pores or PMMA/BMOF composites, in which the inner pores of BMOF are partly blocked by PMMA, we found much lower Li storage capacity (Figs. S11 and S12).
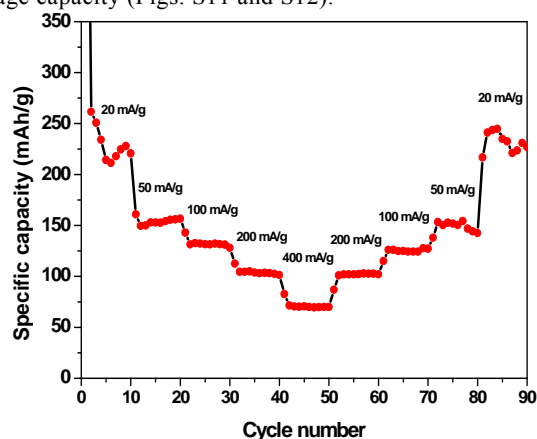

30

Fig. 4 Rate cycling performance of the electrode made with the BMOF discharged at various current densities.

In summary, a new functionalized MOF with remarkable thermal and chemical stability has been designed and

35 synthesized. The functionalized pores result in a good Li storage capacity with high coulombic efficiency. It presents an excellent example for reversible Li storage in stable MOFs via the adsorption mechanism. Ideally, the Li storage capacity can be further improved by increasing the amount of active N-

40 rich functionality and surface area/pore volume.

Acknowledgements

Notes and references

Ningbo Institute of Materials Technology and Engineering, Chinese Academy of Sciences, Ningbo, Zhejiang 315201, China. E-mail:

50 *chenliang@nimte.ac.cn, kongchl@nimte.ac.cn, shencai@nimte.ac.cn,*
†Electronic Supplementary Information (ESI) available: Experimental details, Calculation details, Figs. S1-12. See DOI:10.1039/b000000x/

1   (a) Mulfort, K. L.; Farha, O. K.; Stem, C. L.; Sarjeant, A. A.; Hupp, J. T. *J. Am. Chem. Soc.* 2009, **131**, 3866. (b) Gadzikwa, T.; Farha, O.

55   K.; Malliakas, C. D.; Kanatzidis, M. G.; Hupp, J. T.; Nguyen, S. T. *J. Am. Chem. Soc.* 2009, **131,** 13613.

2   (a) Li, J. R.; Kuppler, R. J.; Zhou, H. C., *Chem. Soc. Rev.* 2009, **38**, 1477. (b) Serra-Crespo, P.; Ramos-Fernandez, E. V.; Gascon, J.; Kapteijn, F. *Chem. Mater.* 2011**, 23**, 2565. (c) Lin, Y.; Kong, C.;

60   Chen L. *RSC Adv.* 2012, **2**, 6417. (d) Vaidhyanathan, R.; Iremonger, S. S.; Dawson, K. W.; Shimizu, G. K. H. *Chem. Commun.* 2009, 5230.

3   (a) Férey, G.; Millange, F.; Morcrette, M.; Serre, C.; Doublet, M.-L.; Greneche, J.-M.; Tarascon J.-M., *Angew. Chem. Int. Ed* 2007, **46**,

65   3259. (b) Li, X.; Cheng, F.; Zhang, S.; Chen, J., *J. Power Sources* 2006, **160**, 542. (c) Saravanan, K.; Nagarathinam, M.; Balaya, P.; Vittal, J. J. *J. Mater. Chem.* 2010, **20**, 8329. (d) Liu, Q.; Yu, L.; Wang, Y.; Ji, Y.; Horvat, J.; Cheng, M.-L.; Jia, X.; Wang, G. *Inorg. Chem.* 2013, **52,** 2817.

70 4   (a) Uemura, T.; Kitaura, R.; Ohta, Y.; Nagaoka, M.; Kitagawa, S. *Angew. Chem. Int. Ed.* 2006, **45**, 4112. (b) Henschel, A.; Gedrich, K.; Kraehnert, R.; Kaskel, S. *Chem. Commun.* 2008, 4192.

5   (a) Férey, G. *Chem. Soc. Rev.* 2008, **37**, 191. (b) Wang, Z. Q.; Cohen, S. M. *J. Am. Chem. Soc.* 2007, **129**, 12368.

75 6   (a) Greathouse, J. A.; Allendorf, M. D. *J. Am. Chem. Soc.*, 2006, **128**, 10678. (b) Dinca, M.; Han, W. S.; Liu, Y.; Dailly, A.; Brown, C. M.; Long, J. R. *Angew. Chem. Int. Ed.* 2007, **46**, 1419. (c) Keskin, S.; van Heest, T. M.; Sholl, D. S. *ChemSusChem* 2010, **3**, 879.

7   (a) Mulfort, K. L.; Farha, O. K.; Stem, C. L.; Sarjeant, A. A.; Hupp,

80   J. T. *J. Am. Chem. Soc.* 2009, **131**, 3866. (b) Wang, Z.; Cohen, S. M., *Chem. Soc. Rev.* 2009, **38**, 1315. (c) Zhang, J.-P.; Zhu, A.-X.; Lin, R.-B.; Qi, X.-L.; Chen, X.-M. *Adv. Mater.* 2011, **23**, 1268.

8   (a) Wu, T. J.; Shen, L. J.; Luebbers, M.; Hu, C.; Chen, Q. M.; Ni Z., Masel, R. I. *Chem. Commun.* 2010, **46,** 6120.（b）Nguyen, J. G.;

85   Cohen, S. M. *J. Am. Chem. Soc.* 2010, **132**, 4560. c) Yang, J.; Grzech, A.; Mulderb, F. M.; Dingemans, T. J. *Chem. Commun.* 2011, **47**, 5244.

9   (a) Banerjee, R.; Furukawa, H.; Britt, D.; Knobler, C.; Ökeeffe, M.; Yaghi, O. M. *J. Am. Chem. Soc.* 2009, **131**, 3875. (b) Morris, W.;

90   Leung, B.; Furukawa, H.; Yaghi, O. K.; He, N.; Hayashi, H.; Houndonougbo, Y.; Asta, M.; Laird, B. B.; Yaghi, O. M. *J. Am. Chem. Soc.* 2010, **132**, 11006.

10 Banerjee, R.; Phan, A.; Wang, B.; Knobler, C.; Furukawa, H.; O'Keeffe, M.; Yaghi. O. M. *Science* 2008, **319**, 939.

95 11   (a) Bauer, S.; Serre, C.; Devic, T.; Horcajada, P.; Marrot, J.; Férey, G.; Stock, N. *Inorg. Chem.* 2008, **47**, 7568. (b) Sonnauer, A.; Stock, N. *Eur. J. Inorg. Chem.* 2008, 5038.

12 Bernt, S.; Guillerm, V.; Serre, C.; Stock, N.; *Chem. Commun.* 2011, **47**, 2838.

100 13 Côté, A. P.; Benin, A. I.; Ockwig, N. W.; O'Keefe, M.; Matzger, A. J.; Yaghi, O. M. *Science* 2005, **310**, 1166.

14 Vermoortele, F; Ameloot, R.; Vimont, A.; Serre, C.; Vos, D. *Chem. Commun.* 2011, 1521.

ChemComm Accepted Manuscript